DOI 10.1007/s10946-020-09860-2
Journal of Russian Laser Research, Volume 41, Number 2, March, 2020

LASER-ASSISTED SPIN COATING OF Al-DOPED ZnO THIN FILMS

Mahira Ismael,* Eman Saied, and Yousif M. Hassan

Department of Physics, Salahaddin University
Erbil, Kurdistan Region, Republic of Iraq

*Corresponding author e-mail: mahera.esmaeel1@su.edu.krd

Abstract

Undoped and aluminum-doped ZnO (AZO) thin films were prepared by the sol–gel process. Single thin layers were synthesized at room temperature by spin coating on glass and silicon substrates. The gel was laser irradiated (530 nm, 10 W) during the spinning process. We used Fourier-transform infrared (FTIR) spectroscopy and scanning electron microscopy (SEM) to characterize the chemical bonding configuration and surface morphology. UV–Vis spectroscopy was used to find optical transmittance, and energy-dispersive X-ray spectroscopy (EDS) was used to measure the surface chemical composition. Results of the EDS and FTIR analyses confirmed the successful preparation of ZnO and AZO through laser-assisted spin coating. SEM images showed that surface morphology and porosity were affected by the doping concentration. Al-doped samples showed high transmittance and possessed optical band gap values between 3.26 and 3.34 eV without laser irradiation and 3.3 – 3.341 eV with laser irradiation. Laser irradiation improved the structure and optical properties of the films.

Keywords: laser irradiation, spin coating, aluminum-doped zinc oxide (AZO), Fourier-transform infrared (FTIR) spectroscopy, thin film.

1. Introduction

Metal-oxide-conducting thin films, such as indium-doped tin-oxide (ITO), indium-oxide, and zinc-oxide transparent conducting films, have great value in making electrical and optical windows for devices. The nontoxicity and abundance of ZnO on the Earth surface make it a perfect material as transparent electrical top contact for solar cells in thin layers. Doping of ZnO films with trivalent or pentavalent element improves their electrical conductivity. ITO thin films exhibit high transparency and high electrical conductivity, but these films are costly due to doping of rare-earth indium and low stability in hydrogen plasma.

A ZnO-based thin film deposited on glass is a good candidate to replace expensive ITO films because of their electrical conductivity, optical transparency, low cost, and good stability in different environments. The conductivity and transparency of ZnO films could be improved by optimizing the doping level and deposition parameters. ZnO thin films would be an attractive alternative to replace ITO for applications in devices such as photovoltaic devices, gas sensors, and transparent conductors [1–3].

It is well known that ZnO is a direct wide-band-gap (3 – 37 eV) semiconductor with high excitonic binding energy (60 meV) at room temperature [3–6]. Scholars have developed extrinsic ZnO-based thin films doped with different elements such as indium (In), aluminum (Al), tin (Sn), gallium (Ga), and manganese (Mn) [7, 8].

Manuscript submitted by the authors in English first on December 17, 2019 and in final form on January 23, 2020.

In addition to doping elements, the increasing of dopant concentration influences the crystallite size and film thickness [7,9]; moreover, the resistivity of intrinsic ZnO thin films can be decreased by Al doping up to 1%. Aluminum-doped zinc oxide (AZO) films display high transparency and low resistivity and are suitable for making transparent electrodes in optical devices, gas sensors, and ultrasonic oscillators [10,11]. Metal-oxide films are deposited by different methods such as sol–gel deposition [12], chemical vapor deposition [13], and atomic layer deposition [14].

In this study, undoped and 1%, 3%, and 5% Al-doped ZnO thin films were coated onto the glass and silicon substrate surface using laser-assisted spin coating. We investigated he effects of Al doping and laser irradiation on the film morphology, chemical bonding, optical transmittance, and chemical composition, using scanning electron microscopy (SEM), Fourier-transform infrared (FTIR) spectroscopy, UV–Vis spectroscopy, and energy-dispersive X-ray (EDX) spectroscopy.

2. Materials and Methods

Glass and silicon sheets (15×15 mm) are used as substrates. Before deposition of the film, the substrates were sequentially washed with ethanol and acetone, then rinsed in distilled water, and dried to remove dirt, oil, or grease. Undoped and Al-doped ZnO films were prepared by laser-assisted spin coating of colloidal suspensions containing different Al concentrations on glass substrates. A green laser ($\lambda =$ 532 nm, $p = 10$ W) is used during deposition on the surface of the films. A ZnO precursor solution was prepared by dissolving zinc acetate [$Zn(CH_3CO_2)_2$] in a solution of ethanol and monoethanolamine (MEA) at room temperature. Ethanol and MEA were used as a solvent and stabilizer, respectively. The molar ratio of MEA to zinc acetate was kept at 1.0, and the concentration of zinc acetate was 0.1 M. The prepared solutions for the pure ZnO were kept under continuous magnetic stirring for 2 h at 70°C until a clear and homogeneous solution was obtained (Fig. 1). The precursor solution was aged for 15 days at room temperature. Al doping was conducted by adding aluminum chloride hexahydrate ($AlCl_36{\cdot}H_2O$) solution in the parent solution. The Al/Zn ratio in the solution changed from 1% to 5%. Spin coating was used at room temperature and at a revolution of 3,000 rpm for 30 s. The deposited film was preheated at 300°C ± 5 °C for 10 min. The coating process was repeated three times to obtain uniform films.

Chemical composition was analyzed using FTIR300 (Mattson Instruments, Inc.), which operates in the 400 – 4000 cm^{-1} mid-infrared region. Optical properties were measured using a Shimadzu UV–Vis-

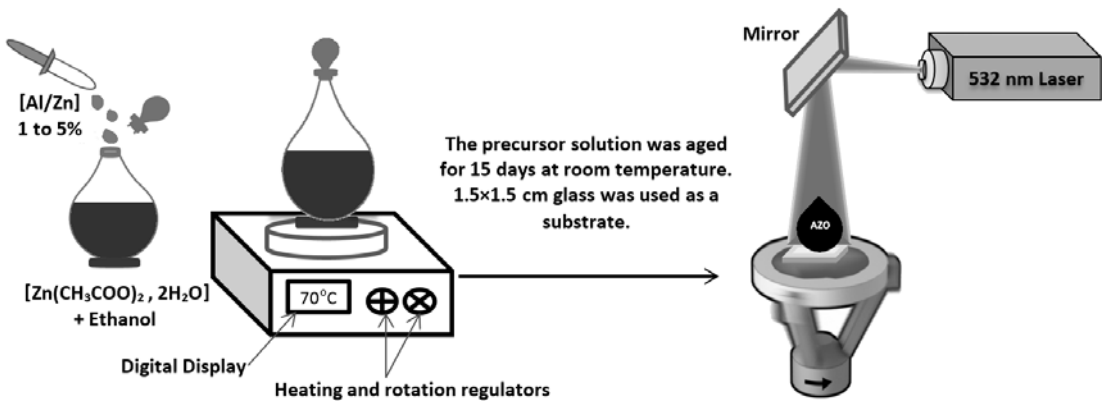

Fig. 1. Preparation steps of AZO thin films by the spin coating method.

mini 1240 spectrophotometer within the wavelength range of 200–1100 nm. Surface morphology of the films was evaluated through fast-emission scanning electron microscopy (Cam Scan MV2300). The chemical composition of the deposited films was determined by the energy-dispersive X-ray spectroscopy (EDS) performed in SEM.

2.1. Chemical Analysis Using FTIR

FTIR spectra were used to analyze the presence of functional groups in molecules. Figure 2 shows the FTIR spectrum of AZO thin films. The spectra consist of various absorption bands within 2400 – 400 cm^{-1}. The stretching vibration of the Zn–O bond is reflected by a peak at 400 – 500 cm^{-1} [15–19]. The broad band at 611.28 cm^{-1} is due to the local vibration of the substituted carbon in the Si substrate [20]. The peak at ∼681.37 cm^{-1} is due to the Al–O bond [17]. The peak at ∼ 821.59 cm^{-1} is attributed to Al in ZnO, and the sharp band at 1111.93 cm^{-1} is assigned to Si–O–Si bonds [20, 21]. Bands within 900–1000 cm^{-1} are assigned to Al–Si–O bonds [22]. The stretching mode of vibration bands between 1600 – 1400 cm^{-1} is due to C–O bonds [16]. The absorption peak at ∼2362.31 cm^{-1} is due to CO_2 molecules in air [18].

2.2. UV–Vis Spectrum

We studied the effect of high Al doping on the optical properties of ZnO films. Figure 3 shows the transmission spectra of Al-doped ZnO films with different doping concentrations within 1200 – 200 nm. The evolution of the transmission $T(\lambda)$ in Fig. 3 a, b shows that 3% Al-doped ZnO thin films exhibit high optical transmission in the visible range, which reaches ∼93% compared to that of undoped ZnO.

Figure 3 c, d shows the effect of laser irradiation during the film deposition. The measurement of the

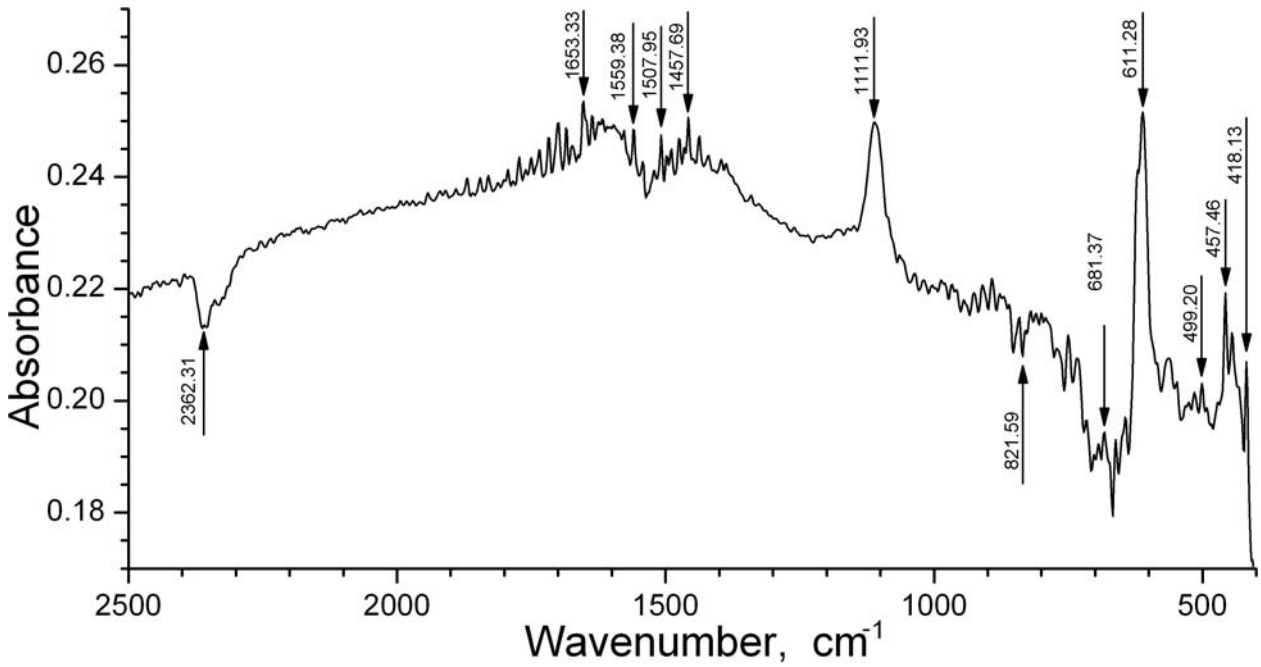

Fig. 2. FTIR spectrum of AZO (5% of Al) thin film prepared by laser-assisted spin coating.

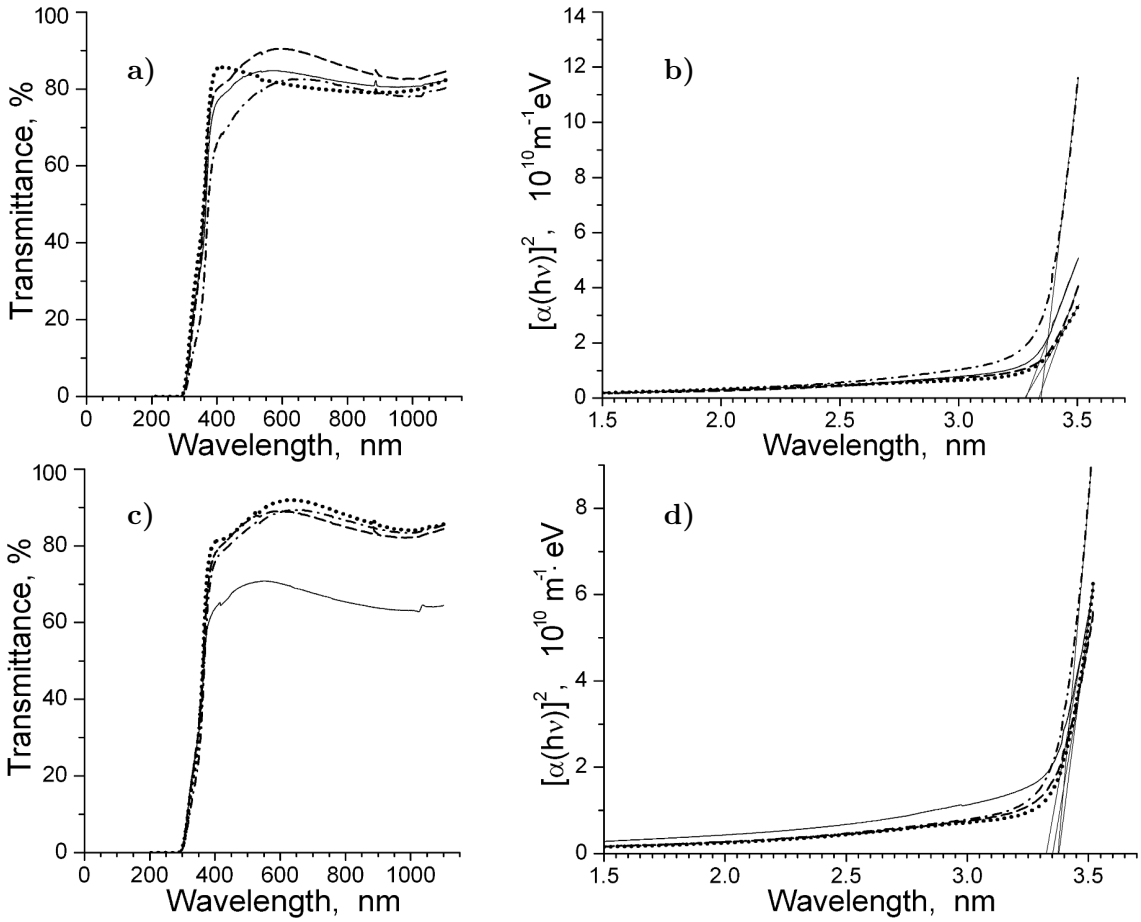

Fig. 3. Transmission (%) versus the wavelength (nm) for ZnO and AZO thin films, and plot of $(\alpha h\nu)^2$ versus $h\nu$ for AZO films with Al concentration equal to zero (solid curve), 1% (dotted curve), 3% (dashed curve), and 5% (dash-dotted curve), without laser irradiation (a, b), and with laser irradiation (c, d).

transmission $T(\lambda)$ shows that Al-doped (at 1%) ZnO films have good optical transmission in the visible range, which can reach 93% compared to that of undoped ZnO. The optical transmission decreases with increase of dopant level to 5%. This result agrees with the crystalline degradation observed in the structural properties [23]. To obtain detailed information on transmittance and optical band gaps, we analyzed the dependence of the absorption coefficient on the photon energy in the high-absorption regions. The optical band gap of the films was determined from the absorption spectra, in view of Tauc's relation [24], $(\alpha h\upsilon)^2 = B(E_g - h\nu)$, where α is the absorption coefficient of the film, B is an energy-independent constant between $10^7 - 10^8$ m^{-1}, h is the Planck constant, ν is the frequency of incident photons, and E_g is the optical band gap. The optical band gap of the thin film was obtained by plotting $(\alpha h\nu)^2$ versus photon energy $(h\nu)$, by extrapolating the linear line to the energy axis (Fig. 3 b). The optical band gaps were found to be 3.26, 3.30, 3.318, and 3.34 eV for 0, 1%, 3%, and 5% Al-doped ZnO thin films, respectively; see Table 1. Thin films with high Al concentration exhibited a wider range of optical band gap energy than pure ZnO. The optical-band-gap value increases from 3.26 to 3.34 eV with increase in the Al concentration.

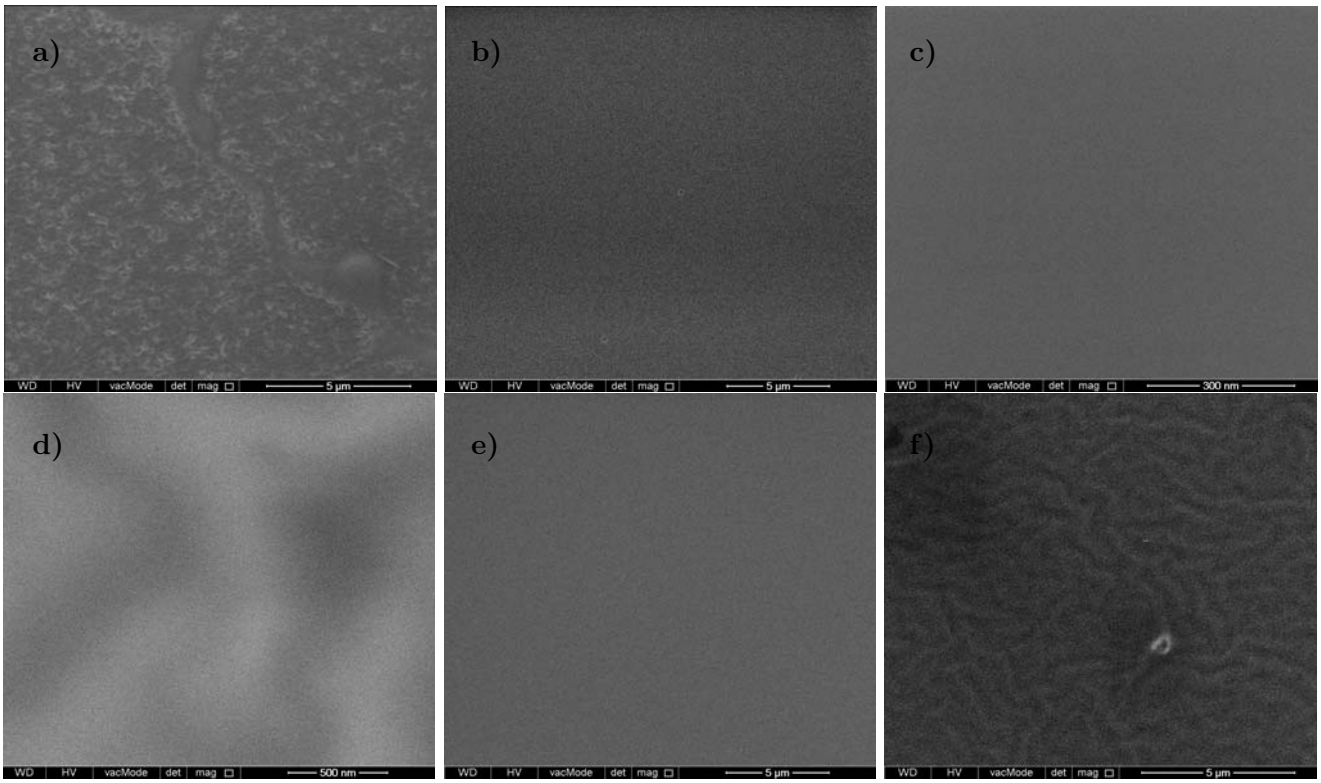

Fig. 4. SEM images (a – d) of AZO of different Al concentrations (0, 1%, 3%, and 5%). The samples were irradiated during preparation; here, pure ZnO and AZO (5%) without laser irradiation (e – f).

The widening of the optical band gap with increasing level of doping is well described by the Burstein–Moss effect [25, 26]. After Al doping, the Al atoms occupy Zn sites in the ZnO lattice. At room temperature, these atoms act as singly-ionized donors, giving one extra electron. These donor electrons occupy the states at the bottom of the conduction band. Therefore, these states are filled with donor electrons with increasing doping concentration, leading to widening of the band gap. This phenomenon is known as the Burstein–Moss shift. When using laser irradiation during deposition, the optical-band gaps are 3.3, 3.322, 3.323, and 3.341 eV for 0, 1%, 3%, and 5% Al-doped ZnO thin films, respectively (Table 1). The laser-irradiated thin films exhibited a wider range of optical band gap energy than the samples not subjected to laser irradiation because of the reduced disorder of the system in the former, as a result of increasing grain size.

Table 1. Energy Gap for ZnO of Different Concentrations of Al:ZnO Films (with and without Laser Irradiation).

Al Concentration %	Energy gap, eV	
	without laser irradiation	with laser irradiation
0	3.26	3.3
1	3.30	3.322
3	3.318	3.323
5	3.34	3.341

2.3. SEM Images and EDS Analysis

Figure 4 a – d shows the SEM images of the surface of Al-doped ZnO films of different Al percentages (i.e., 0, 1%, 3%, and 5%) for a fixed substrate temperature. Some of the films were treated through laser irradiation during film coating. The deposited films have smooth and uniform surfaces. The SEM images show no significant change in the surface morphology of ZnO films with increasing concentration of the Al dopant. Furthermore, the crystal structure of the film improved with increasing Al concentration. The surface morphology of the films was found to be strongly dependent on Al concentration. Figure 4 e, f shows the SEM image of undoped and 5% Al-doped ZnO thin films without laser irradiation. A comparison with Fig. 4 a shows that laser irradiation during deposition improved the surface morphology. It is clear that, after laser exposure, the grain size increases up to the higher value. It was also found that the thickness of the 5% Al-doped ZnO film in the SEM cross-section image is approximately 1000 nm, which was thicker than other films.

Table 2 shows the energy-dispersive X-ray (EDX) results of the ZnO films. The results confirm the presence of Zn, O, and Al atoms in the pure ZnO and the different atomic percentages of Al in doped ZnO thin films, thereby indicating the absence of any other impurities in the samples. Finally, the EDS, FTIR, and SEM analyses confirmed the successful preparation of pure ZnO and AZO through laser-assisted spin-coating. The deposition process and film formation mechanism of Al : ZnO via the laser-assisted spin coating technique is explained in Fig 5.

Table 2. EDX Data of the ZnO Films, Pure and Doped with Different Aluminum Concentrations.

Al Concentration, %	O, %	Al,%	Zn, %
0	52.1	0.05	1.2043
1	56.52	0.607	2.1306
3	47.25	0.38	0.78
5	48.68	0.59	0.71

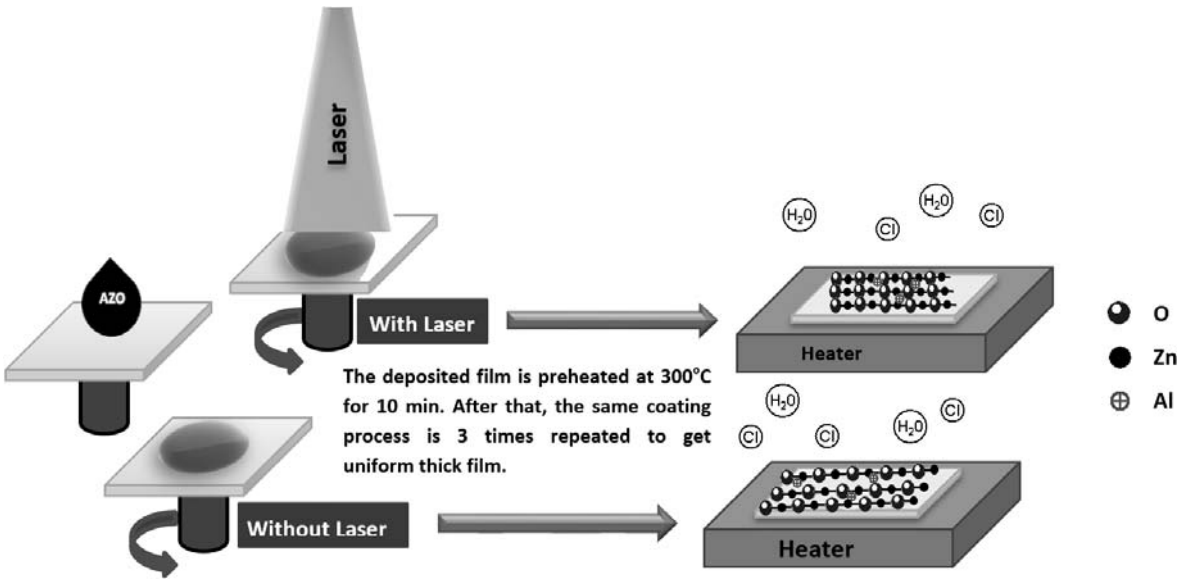

Fig. 5. Deposition process and film formation mechanism of Al : ZnO via the laser-assisted spin coating technique.

3. Summary

In this work, ZnO and AZO films were synthesized by the sol–gel method. Laser irradiation (530 nm, 10 W) was used during preparation. SEM images showed the smooth surface of the films. EDX showed that the oxygen content in the film decreased with increasing aluminum concentration, while Al and Zn fluctuations were observed in the deposited films. The structure and composition of the films were confirmed in the FTIR spectra. The optical transmission spectra showed that the presence of Al in the ZnO lattice improved the transmission in the visible range and increased the optical band gap. Laser irradiation during film coating enhanced the films' transmittance and their crystallites.

References

1. P. Zhang, J. Wu, T. Zhang, et al., *Adv. Mater.*, **3**, 1703737 (2017).
2. T. Shirahata, T. Kawaharamura, and S. Fujita, *Thin Solid Films*, **597**, 30 (2015).
3. L. Zhu and W. Zeng, *Sens. Actuators A: Phys.*, **267**, 242 (2017).
4. T. Jannane, M. Manoua, A. Liba, et al., *J. Mater. Environ. Sci,*, **8**, 160 (2017).
5. Y. Li, L. Xu, X. Li, et al., *Appl. Surf. Sci.*, **256**, 4543 (2010).
6. S. Y. Kuoa, W. C. Chen, F. I. Lai, et al., *J. Cryst. Growth*, **287**, 78 (2006).
7. J. H. Lee and B. O. Park, *Thin Solid Films*, **426**, 94 (2003).
8. X. Hao, J. Ma, D. Zhang, et al., *Appl. Surf. Sci.*, **189**, 18 (2002).
9. Sh. Salam, M. Islam, and M. A. Akram, *Thin Solid Films*, **529**, 242 (2013).
10. H. M. Zhou, D. Q. Yi, Z. M. Yu, et al., *Thin Solid Films*, **515**, 6909 (2007).
11. J. Nishino, T. Kawarada, S. Ohisho, et al., *J. Mater. Sci. Lett.*, **16**, 629 (1997).
12. E. Gutmann, A. Levin, I. Pommrich, and D. Meyer, *Cryst. Res. Technol.*, **40**, 124 (2005).
13. P. Saikia, A. Borthakur, and P. K. Saikia, *Indian J. Phys.*, **85**, 551 (2011).
14. R. Katamreddy, R. Inman, G. Jursich, et al., *Thin Solid Films*, **515**, 6931 (2007).
15. Z. Yamlahi Alam, M. Salem, M. Gaidi, and J. Elkhamkhami, *Adv. Energy: Int. J. (AEIJ)*, **2**, 4, 11 (2015).
16. A. Vanaja, G. V. Ramaraju, and K. Srinivasa Rao, *Indian J. Sci. Technol.*, **9**, 12 (2016).
17. T. Ganesh, K. Perumal, R. Kumar, and N. Bhaskar, *Nano Hybrids Composit.*, **17**, 171 (2017).
18. A. Djelloul, M-S. Aida, and J. Bougdira, *J. Luminescence*, **130**, 2113 (2010).
19. D. Djouadi, A. Chelouche, and A. Aksas, *J. Mater. Environ. Sci.*, **3**, 585 (2012).
20. K. L. Foo, M. Kashif, U. Hashim, and M. E. Ali, *Curr. Nanosci.*, **9**, 000 (2013).
21. M. U. Shahid, K. M. Deen, A. Ahmad, et al., *Appl. Nanosci.*, **6**, 235 (2016).
22. Y. M. Hassan and E. A. Saied, *Indian J Phys.*, **88**, 43 (2014).
23. K. M. Sandeep, S. Bhat, and S. M. Dharmaprakash, *Appl. Phys. A*, **122**, 975 (2016).
24. J. I. Pankove, *Optical Processes in Semiconductors*, Englewoord Cliffs, Prentice-Hall (1971).
25. E. Bursteib, *Phys. Rev.*, **93**, 632 (1954).
26. T. S. Moss, *Proc. Phys. Soc. London B*, **67**, 775 (1954).